Critical-state model for intermodulation distortion in a superconducting microwave resonator

J. McDonald and J. R. Clem
Ames Laboratory and Department of Physics and Astronomy, Iowa State University, Ames, Iowa 50011

D. E. Oates
Lincoln Laboratory, Massachusetts Institute of Technology, Lexington, Massachusetts 02173

(Received 1 December 1997; accepted for publication 10 February 1998)

A model is presented for the treatment of intermodulation distortion in a superconducting transmission line caused by vortex penetration and hysteresis. An analytical framework is developed, and numerical results are presented for center conductors of both circular and rectangular thin-film cross section. © *1998 American Institute of Physics.* [S0021-8979(98)03510-5]

I. INTRODUCTION

There is presently considerable interest in the use of high-temperature superconductors (HTSs) in passive microwave devices such as filters for wireless communication.[1–4] Much of this interest stems from the fact that recent prototypes of HTS filters have shown performance superior to conventional filters by at least an order of magnitude.[1,4] This improvement is due to the lower conductor loss of HTSs as compared with conventional conductors. Lower conductor loss leads to a larger unloaded Q and, therefore, to a narrower bandwidth.

One drawback to the use of HTSs is their nonlinearity. This nonlinearity manifests itself in a dependence of the surface impedance on the input power or transport current amplitude.[5,6] One consequence of the power dependence is that the low-power surface impedance is no longer a sufficient figure of merit for the material. Instead, the surface impedance must be determined at the specific power at which the device will be operated.[5] Nonlinearities also lead to two-frequency intermodulation (IM). The occurrence of IM in filters can cause various problems such as the generation of spurious targets in radar receivers.[5] A good understanding of these nonlinear effects must be achieved before high-quality filters can be constructed from HTSs. While these effects are present even at lower input powers, they become much more pronounced as the power increases. Experimental evidence suggests that the nonlinearity is associated with the onset of vortex penetration and hysteresis.[5,6] Previous modeling of the data has assumed a coupled-grain model at low input power.[2,7] This model was successful in fitting the behavior of both the resistive and reactive responses of the surface impedance. At higher power a modified Bean model was employed.[2] This model was able to quantitatively explain the power dependence of the surface resistance. Thus far, models to explain IM in either the low-power or high-power regions have been lacking.[2]

The purpose of this article is to provide a model for describing IM due to quasistatic vortex penetration and hysteresis. We will employ a field-independent critical-state model with the assumption that $H_{c1}=0$ (Bean model).[8] This should be an excellent approximation when the average self-field is larger than H_{c1}. We will also neglect any effects due to surface barriers.[9]

II. THE MODEL

We consider a one-dimensional coaxial-type transmission line. The outer conductor is a superconducting cylindrical shell of radius R. The inner conductor is either a superconducting wire of circular cross section with radius r, or a superconducting thin-film strip of width $2W$ and thickness d (see Fig. 1). The input signal contains two closely spaced frequencies ω_1 and ω_2 centered around the resonant frequency ω_0. The resulting transport current in the center conductor I_T is given by

$$I_T(t)=\frac{I_{T0}}{2}\left[\cos(\omega_1 t)+\cos(\omega_2 t)\right], \tag{1}$$

which can also be written as

$$I_T(t)=I_{T0}\cos(\omega_0 t)\cos(\Delta\omega t), \tag{2}$$

where $\omega_1=\omega_0+\Delta\omega$ and $\omega_2=\omega_0-\Delta\omega$. We assume that for the circular geometry $\lambda \ll r$, and that for the strip geometry either $\lambda<d\ll W$ or $d<\lambda<\Lambda\ll W$, where λ is the London penetration depth and $\Lambda=2\lambda^2/d$ is the two-dimensional screening length.[10] For the strip geometry we will also assume that R is large enough that the center conductor can be treated as if it were isolated. This turns out not to be very restrictive.[11–13] These assumptions allow us to use the well-known results for infinitely long, isolated circular wires and strips.[14–16]

When I_{T0} becomes large enough, vortices will start to penetrate into the center conductor from its surface. In our calculations we assume that $H_{c1}=0$ and that there are no surface barriers, so vortex penetration occurs for all $I_{T0}>0$. For the circular geometry the vortices will be closed circular rings, while for the strip geometry they will be either Abrikosov ($\lambda<d$) or Pearl ($d<\lambda$) vortices. For simplicity we will neglect any vortex penetration in the outer conductor. We assume that we can treat the vortex motion quasistatically. This will be done using a critical-state model with field-independent J_c.[14–16]

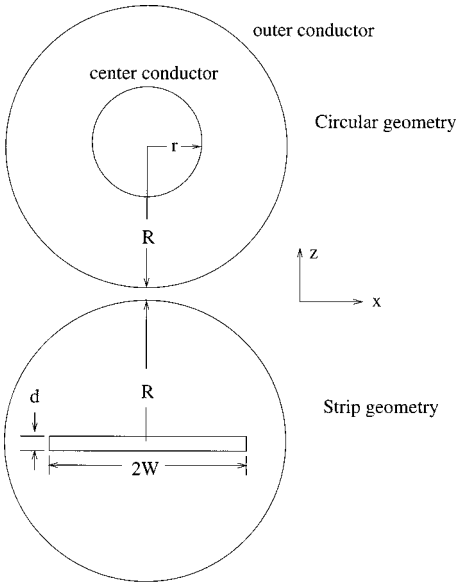

FIG. 1. The two geometries considered in this paper. The outer conductor is a cylindrical shell of radius R. The center conductor is either a circular wire of radius r or a thin-film strip of width $2W$ ($W \ll R$) and thickness d. The y axis points into the page.

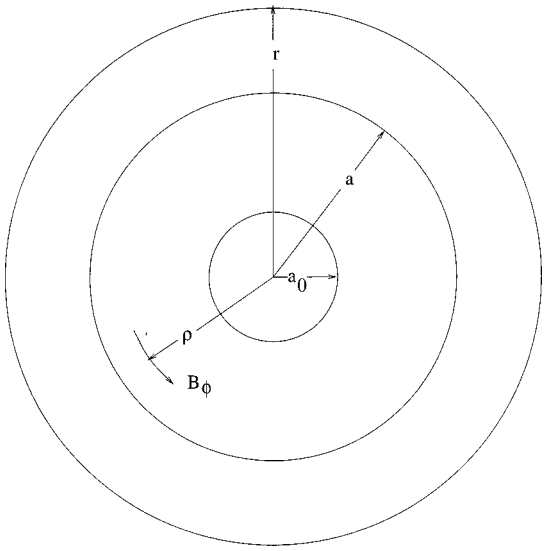

FIG. 2. Cross section of the center conductor for the circular geometry. The radius of the moving flux front is a. The flux density B_ϕ changes only in the region $\rho > a$. The region $\rho < a_0$ is completely screened with $B_\phi = 0$ and $J_y = 0$.

The voltage drop per unit length is given by Faraday's law

$$V(t) = \frac{d}{dt}\,\Phi(t), \tag{3}$$

where $\Phi(t)$ is the magnetic flux per unit length enclosed between the axis of the transmission line and the outer conductor. Therefore, to calculate $V(t)$ we must first determine the magnetic field generated by the transport current.

The current-density and flux-density profiles may be determined using the critical-state model. The critical state in the presence of two frequencies is considerably more complicated than for a single frequency, but the theoretical analysis is considerably simplified if we make the assumption $\omega_0/\Delta\omega = N = \text{integer}$. When this is true, $I_T(t)$ is periodic with period $T = 2\pi/\Delta\omega$; therefore, $V(t)$ is also periodic with the same period. We may, therefore, express $V(t)$ as a Fourier series

$$V(t) = I_{T0} \sum_{n=1}^{\infty} [R_n \cos(n\Delta\omega t) - X_n \sin(n\Delta\omega t)], \tag{4}$$

where the coefficients R_n and X_n are given by

$$R_n = \frac{\Delta\omega}{\pi I_{T0}} \int_0^T dt\, V(t) \cos(n\Delta\omega t), \tag{5}$$

and

$$X_n = \frac{-\Delta\omega}{\pi I_{T0}} \int_0^T dt\, V(t) \sin(n\Delta\omega t), \tag{6}$$

respectively. Since $\omega_1 = (N+1)\Delta\omega$ and $\omega_2 = (N-1)\Delta\omega$, the fundamental response will be given by the $n = N+1$ and $n = N-1$ terms in the series. The third-order intermodulation response, at frequencies $2\omega_1 - \omega_2$ and $2\omega_2 - \omega_1$, is given by the $n = N+3$ and $n = N-3$ terms of the series. The time-averaged dissipated power per unit length is given by

$$P_{\text{diss}} = \frac{1}{T} \int_0^T I_T(t) V(t)\, dt. \tag{7}$$

Inserting Eq. (1) and Eq. (3) into Eq. (4) yields

$$P_{\text{diss}} = \frac{I_{T0}^2}{4} (R_{N+1} + R_{N-1}). \tag{8}$$

Equation (8) implies that the resistance per unit length of the transmission line is equal to the average of R_{N+1} and R_{N-1}. The reactance per unit length is equal to the average of X_{N+1} and X_{N-1}.

We first consider the circular geometry. In a circular wire, flux will penetrate in from the surface as circular fronts. There will only be one flux front moving at a time. Let $a(t)$ be the radius of this front (see Fig. 2). The voltage drop per unit length $V(t)$ is given by

$$V(t) = \frac{d}{dt}\left[\int_0^R d\rho B_\phi(\rho,t)\right] = \frac{da}{dt}\left[\int_0^R d\rho\, \frac{\partial}{\partial a} B_\phi(\rho,a)\right], \tag{9}$$

where $B_\phi(\rho,t)$ is the magnetic flux density at radius ρ measured from the center of the wire. The expression for the magnitude of the partial derivative of B_ϕ is given by

$$\left|\frac{\partial}{\partial a} B_\phi(\rho,a)\right| = \begin{cases} 0, & \rho < a, \\ 2\mu_0 J_c a/\rho, & a < \rho, \end{cases} \tag{10}$$

and the sign is opposite to the sign of the current density in the region $a < \rho < r$. The magnitude of $V(t)$ is given by

$$|V(t)| = -2\mu_0 J_c a \frac{da}{dt} \ln\left(\frac{R}{a}\right), \tag{11}$$

and the sign of $V(t)$ is the same as the sign of the current in the region $a<\rho<r$. Therefore, once $a(t)$ is determined, $V(t)$ can be calculated with Eq. (11).

To determine $a(t)$ we must examine the equation

$$\frac{d}{dt} I_T(t)=0. \tag{12}$$

The roots of Eq. (12) are the values of t at which the previous flux front stops moving and the new flux front starts to penetrate in from the surface. Using Eq. (1) for $I_T(t)$ in Eq. (12) yields a transcendental equation which can only be solved numerically. However, when $N\gg 1$, the roots deviate only very slightly from integer multiples of π/ω_0. Using this approximation for the roots of Eq. (12) allows us to derive the expressions for $a(t)$. In order to derive the expressions we divide up the period $T=2\pi/\Delta\omega$ into four equal intervals. Each of these intervals is then divided into $N/2$ equal subintervals. Each subinterval corresponds to a time period π/ω_0. At $t=0$ the center conductor has current-density and flux-density profiles given by

$$J_y(\rho)=\begin{cases} 0, & \rho<a_0, \\ J_c & a_0<\rho<r, \end{cases} \tag{13}$$

and

$$B_\phi(\rho)=\begin{cases} 0, & \rho<a_0, \\ \dfrac{\mu_0 J_c(\rho^2-a_0^2)}{2\rho}, & a_0<\rho<r, \\ \dfrac{\mu_0 J_c(r^2-a_0^2)}{2\rho}, & r<\rho<R, \end{cases} \tag{14}$$

where $a_0=\sqrt{1-F}$ and $F=I_{T0}/I_c$ with $I_c=\pi r^2 J_c$. A new front begins to penetrate in from the surface at $t=0$ and collapses quasistatically toward the center until $t=\pi/\omega_0$, at which time it stops at radius $a_1>a_0$. This new front leaves a current density $-J_c$ behind it as it penetrates in. At time $t=\pi/\omega_0$ another front begins to penetrate in and leaves a current density $+J_c$ behind it. This front stops at time $t=2\pi/\omega_0$ and radius $a_2>a_1$. This process continues until $t=(N/2-1)\pi/\omega_0$, at which time there is a remnant structure consisting of annular regions with the current density alternating between $+J_c$ and $-J_c$. The outermost annular region contains a current density $-J_c$. At time $t=(N/2-1)\pi/\omega_0$, a new front begins to penetrate into this remnant structure, leaving a current density $+J_c$ behind, and it stops at time $t=(N/2+1)\pi/\omega_0$. At time $t=(N/2+1)\pi/\omega_0$, a front begins to penetrate in, leaving a current density $-J_c$, and stops at time $t=(N/2+2)\pi/\omega_0$. This process continues until $t=N\pi/\omega_0$, at which time the current density is the same as as in Eq. (13) except with a negative sign. This corresponds to time $t=T/2$. The same process occurs between $t=T/2$ and $t=T$, except that the positive and negative current densities are switched. The expression for $a(t)$ is derived by writing the expression for $I_T(t)$ in terms of $a(t)$ in each subinterval. The resulting expression for the first interval $0\leqslant t<T/4$ is given by

$$a(t)/r=\sqrt{1-\frac{F}{2}\left[\cos\left(\frac{m\pi}{N}\right)+(-1)^{m+1}I_T(t)/I_{T0}\right]}, \tag{15}$$

where m is the index that labels the subintervals, $m\pi\leqslant\omega_0 t<(m+1)\pi$, $m=0,1,...,N/2-1$. The expression for $I_T(t)$ is given by either Eq. (1) or Eq. (2). For $T/4\leqslant t<T/2$, the expressions are

$$a(t)/r=\begin{cases} \sqrt{1-\dfrac{F}{2}\left[\sin\left(\dfrac{m\pi}{N}\right)+(-1)^m I_T(t)/I_{T0}\right]}, & (-1)^m I_T(t)/I_{T0}<\sin\left(\dfrac{m\pi}{N}\right), \\ \sqrt{1-\dfrac{F}{2}\left[\sin\left(\dfrac{(m+1)\pi}{N}\right)+(-1)^m I_T(t)/I_{T0}\right]}, & \text{otherwise}, \end{cases} \tag{16}$$

$(N/2+m)\pi\leqslant\omega_0 t<(N/2+m+1)\pi$, $m=0,1,...,N/2-1$. The reason that there are two expressions for $T/4\leqslant t<T/2$ is that the flux fronts are penetrating through a remnant state. For $T/2\leqslant t<3T/4$,

$$a(t)/r=\sqrt{1-(F/2)[\cos(m\pi/N)+(-1)^m I_T(t)/I_{T0}]}, \tag{17}$$

$(N+m)\pi\leqslant\omega_0 t<(N+m+1)\pi$, $m=0,1,...,N/2-1$. For $3T/4\leqslant t<T$,

$$a(t)/r=\begin{cases} \sqrt{1-\dfrac{F}{2}\left[\sin\left(\dfrac{m\pi}{N}\right)+(-1)^{m+1} I_T(t)/I_{T0}\right]}, & (-1)^{m+1} I_T(t)/I_{T0}<\sin\left(\dfrac{m\pi}{N}\right), \\ \sqrt{1-\dfrac{F}{2}\left[\sin\left(\dfrac{(m+1)\pi}{N}\right)+(-1)^{m+1} I_T(t)/I_{T0}\right]}, & \text{otherwise}, \end{cases} \tag{18}$$

$(3N/2+m)\pi \leqslant \omega_0 t < (3N/2+m+1)\pi, \quad m=0,1,...,N/2-1.$
Using these expressions to calculate da/dt, we obtain

$$V(t) = -\frac{\mu_0 I_{T0}}{4\pi}\left(\omega_1 \sin(\omega_1 t) + \omega_2 \sin(\omega_2 t)\right) \times \left[\ln\left(\frac{R}{r}\right) - \ln\left(\frac{a(t)}{r}\right)\right]. \tag{19}$$

The first term within the brackets is a linear inductive response and is proportional to the geometric reactance per unit length X_0,

$$X_0 = \frac{\mu_0 \omega_0}{2\pi}\ln\left(\frac{R}{r}\right). \tag{20}$$

The second term arises from the hysteretic behavior and leads to nonlinearities.

A similar analysis can be applied to the strip geometry. Let the position of the moving front be given by $a(t)$ (see Fig. 3). The voltage drop per unit length is given by

$$V(t) = \frac{d}{dt}\left[-\int_0^R dx B_z(x,t)\right] = \frac{da}{dt}\left[-\int_0^R dx \frac{\partial}{\partial a} B_z(x,a)\right], \tag{21}$$

where B_z is the normal component of the magnetic field in the $x-y$ plane a distance x from the center of the strip. The magnitude of the partial derivative of B_z is given by

$$\left|\frac{\partial}{\partial a} B_z(x,a)\right| = \begin{cases} 0, & x<a, \\ B_f \dfrac{2a}{\sqrt{(W^2-a^2)(x^2-a^2)}}, & x>a, \end{cases} \tag{22}$$

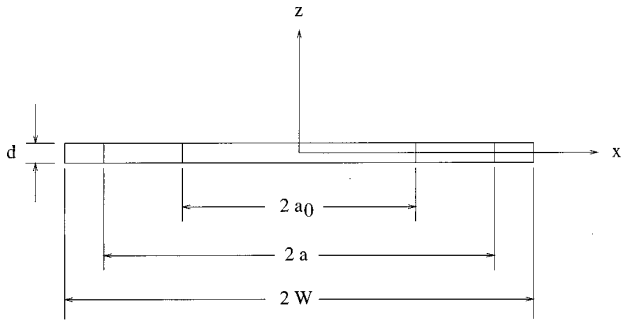

FIG. 3. Cross section of the center conductor for the strip geometry. The flux density B_z changes only in the outer regions $a<|x|<W$. The region $|x|<a_0$ is completely screened with $B_z=0$.

where the scaling field B_f is given by[16]

$$B_f = \frac{\mu_0 J_c d}{\pi}, \tag{23}$$

and the sign is the same as the sign of the current density in the region $a<x<W$. The magnitude of $V(t)$ is

$$|V(t)| = -2B_f a \frac{da}{dt}\frac{1}{\sqrt{W^2-a^2}}\ln\left(\frac{R+\sqrt{R^2-a^2}}{a}\right), \tag{24}$$

and the sign is the same as the sign of the current density in the region $a<x<W$.

The period is divided and subdivided in the same way as for the circular geometry. The expression for $a(t)$ during the first interval $0 \leqslant t < T/4$ is given by

$$a(t)/W = \sqrt{1-(F^2/4)[\cos(m\pi/N)+(-1)^{m+1}I_T(t)/I_{T0}]^2}, \tag{25}$$

$m\pi \leqslant \omega_0 t < (m+1)\pi, \ m=0,1,...,N/2-1$. For $T/4 \leqslant t < T/2$,

$$a(t)/W = \begin{cases} \sqrt{1-\dfrac{F^2}{4}\left[\sin\left(\dfrac{m\pi}{N}\right)+(-1)^m I_T(t)/I_{T0}\right]^2}, & (-1)^m I_T(t)/I_{T0} < \sin\left(\dfrac{m\pi}{N}\right), \\ \sqrt{1-\dfrac{F^2}{4}\left[\sin\left(\dfrac{(m+1)\pi}{N}\right)+(-1)^m I_T(t)/I_{T0}\right]^2}, & \text{otherwise}, \end{cases} \tag{26}$$

$(N/2+m)\pi \leqslant \omega_0 t < (N/2+m+1)\pi, \ m=0,1,...,N/2-1$. For $T/2 \leqslant t < 3T/4$,

$$a(t)/W = \sqrt{1-(F^2/4)[\cos(m\pi/N)+(-1)^m I_T(t)/I_{T0}]^2}, \tag{27}$$

$(N/2+m)\pi \leqslant \omega_0 t < (N+m+1)\pi, \ m=0,1,...,N/2-1$. For $3T/4 \leqslant t < T$,

$$a(t)/W = \begin{cases} \sqrt{1-\dfrac{F^2}{4}\left[\sin\left(\dfrac{m\pi}{N}\right)+(-1)^{m+1} I_T(t)/I_{T0}\right]^2}, & (-1)^{m+1} I_T(t)/I_{T0} < \sin\left(\dfrac{m\pi}{N}\right), \\ \sqrt{1-\dfrac{F^2}{4}\left[\sin\left(\dfrac{(m+1)\pi}{N}\right)+(-1)^{m+1} I_T(t)/I_{T0}\right]^2}, & \text{otherwise}, \end{cases} \tag{28}$$

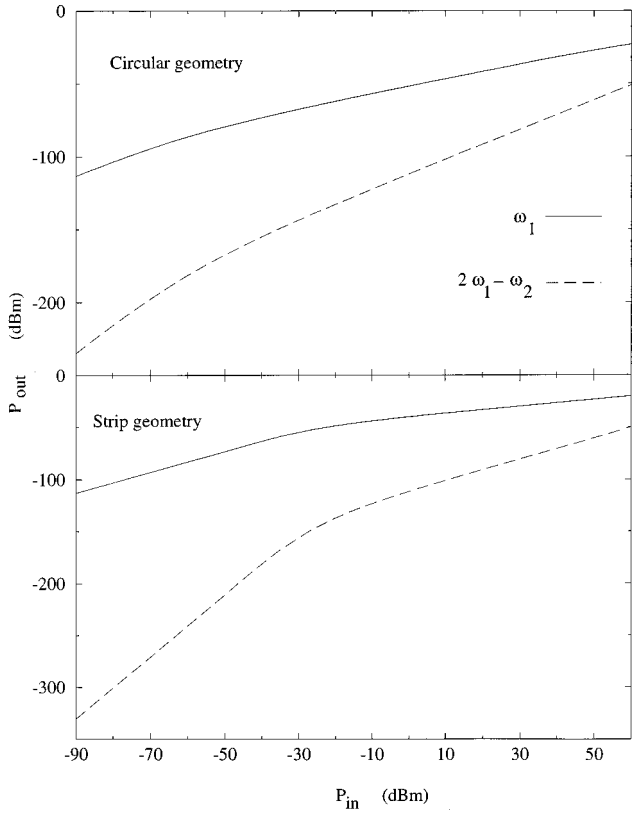

FIG. 4. P_{out} vs P_{in} for a resonator, with either circular (top) or strip (bottom) center conductor, at frequencies ω_1 and $2\omega_1-\omega_2$. The parameter values used were $Z_0=50\ \Omega$, $f_0=\omega_0/2\pi=1.6$ GHz, $l=3$ cm, W or $a=75\ \mu$m, $d=0.3\ \mu$m, and $J_c=10^6$ A/cm^2. It was assumed that the dielectric constant characterizing the region between the conductors is $\epsilon=10$.

$(3N/2+m)\pi \lesssim \omega_0 t < (3N/2+m+1)\pi, \quad m=0,1,...,N/2-1.$ Using these expressions to calculate da/dt, we obtain

$$V(t)=-\frac{\mu_0 I_{T0}}{4\pi}\left[\omega_1 \sin(\omega_1 t)+\omega_2 \sin(\omega_2 t)\right] \times \ln\left(\frac{R+\sqrt{R^2-a^2}}{a}\right). \tag{29}$$

If we expand around large R, the result is

$$V(t)=-\frac{\mu_0 I_{T0}}{4\pi}\left[\omega_1 \sin(\omega_1 t)+\omega_2 \sin(\omega_2 t)\right] \times \left[\ln\left(\frac{2R}{W}\right)-\ln\left(\frac{a(t)}{W}\right)+O\left(\frac{W^2}{R^2}\right)\right]. \tag{30}$$

The first term is proportional to the geometric reactance per unit length

$$X_0 \simeq \frac{\mu_0\omega_0}{2\pi}\ln\left(\frac{2R}{W}\right). \tag{31}$$

The second term arises from the hyteretic behavior and leads to nonlinearities. The third term leads to small corrections and will be neglected.

Resonators have a finite length. Therefore, if we want to apply our results to a resonator we must assume that the fringing effects due to the ends of the resonator can be neglected, and we must multiply our expression for $V(t)$ by the resonator length ℓ to make it dimensionally correct. In a typical experiment a current given by Eq. (1) is established in the center conductor. The input power is the same for both frequencies.[2] The output voltage signal is analyzed to determine the distribution of power among the various frequencies inside the resonator. The amount of output power at a given frequency can then be plotted versus the input power to determine the degree of nonlinearity present. The relation between the time-averaged available incident power P_{inc} and the peak current I_{T0} was derived previously,[17]

$$I_{T0}=\sqrt{\frac{8r_v(1-r_v)QP_{\text{inc}}}{\pi Z_0}}, \tag{32}$$

where Q is the unloaded quality factor and Z_0 is the characteristic impedance of the line. The relation between the time-averaged output power P_{out} and P_{inc} is given by $P_{\text{out}}=r_v^2 P_{\text{inc}}$, where r_v is the voltage insertion ratio. In terms of S parameters, $r_v=|S_{21}|$. This is a power-dependent quantity, which is nearly proportional to Q at intermediate powers.[17] The insertion loss (IL) is given by $\text{IL}=-20\log_{10} r_v$ dB. The output power is distributed among the various frequencies present in the voltage signal. The power spectrum at frequency $n\Delta\omega$ is proportional to $R_n^2+X_n^2$. The amount of output power at frequency $n\Delta\omega$ $[P_{\text{out}}(n\Delta\omega)]$ is given by the product of the time-averaged output power and the fraction of power stored at that frequency,

$$P_{\text{out}}(n\Delta\omega)=P_{\text{out}}\times\left(\frac{R_n^2+X_n^2}{\Sigma_{n'=1}^{\infty}(R_{n'}^2+X_{n'}^2)}\right). \tag{33}$$

Figure 4 shows plots of $P_{\text{out}}(\omega_1)$ and $P_{\text{out}}(2\omega_1-\omega_2)$ vs P_{inc} for both the circular and strip geometries. The parameters chosen were $Z_0=50\ \Omega$, $f_0=\omega_0/2\pi=1.6$ GHz, $\ell=3$ cm, W or $a=75\ \mu$m, $d=0.3\ \mu$m, and $J_c=10^6$ A/cm^2. At low incident powers, the slope of $P_{\text{out}}(\omega_1)$ vs P_{inc} is equal to one for both geometries and the slope of $P_{\text{out}}(2\omega_1-\omega_2)$ is equal to two for the circular geometry and three for the strip geometry. At intermediate incident powers, the slope of $P_{\text{out}}(\omega_1)$ becomes equal to 1/2 for the circular geometry and 1/3 for the strip geometry, while the slope of $P_{\text{out}}(2\omega_1-\omega_2)$ is equal to one for both geometries. The change in slope between the low and intermediate power regions is observed experimentally.[18,19] The third-order intercept (TOI) is equal to 29.0 dBm for the circular geometry and 18.0 dBm for the strip geometry.

III. CONCLUSION

We have presented a critical-state model for intermodulation distortion in a superconducting coaxial-type transmission line. This model can be applied to a superconducting microwave resonator if end effects are neglected. Center conductors of both circular and thin-film cross section were treated. The results presented should be of relevance to experiments dealing with the design and testing of superconducting microwave devices.

ACKNOWLEDGMENTS

Ames Laboratory is operated for the U.S. Department of Energy by Iowa State University under Contract No. W-7405-ENG-82. This research was supported by the Director for Energy Research, Office of Basic Energy Sciences. The work at Lincoln Laboratory was supported by the Air Force Office of Scientific Research, and by the Department of Physics at the Massachusetts Institute of Technology.

[1] G. B. Lubkin, Phys. Today **48**, 20 (1995).
[2] D. E. Oates, P. P. Nguyen, G. Dresselhaus, M. S. Dresselhaus, G. Koren, and E. Polturak, J. Supercond. **8**, 725 (1995).
[3] G.-C. Liang, D. Zhang, C.-F. Shih, M. E. Johansson, R. S. Withers, W. Ruby, D. E. Oates, A. C. Anderson, P. A. Polakos, P. M. Mankiewich, E. DeObaldia, and R. E. Miller, IEEE Trans. Microwave Theory Tech. **43**, 3020 (1995).
[4] Z.-Y. Shen, in *High-Temperature Superconducting Microwave Circuits* (Artech House, Boston, 1994), p. 103.
[5] P. P. Nguyen, D. E. Oates, G. Dresselhaus, M. S. Dresselhaus, and A. C. Anderson, Phys. Rev. B **51**, 6686 (1995).
[6] M. A. Golosovsky, H. J. Snortland, and M. R. Beasley, Phys. Rev. B **51**, 6462 (1995).
[7] S. Sridhar, Appl. Phys. Lett. **65**, 1054 (1994).
[8] C. P. Bean, Phys. Rev. Lett. **8**, 250 (1962).
[9] J. R. Clem, J. Appl. Phys. **50**, 3518 (1979).
[10] J. Pearl, Appl. Phys. Lett. **5**, 65 (1964).
[11] A. M. Campbell, IEEE Trans. Appl. Supercond. **5**, 687 (1995).
[12] S. Fleshler, L. T. Cronis, G. E. Conway, A. P. Malozemoff, T. Pe, J. McDonald, J. R. Clem, G. Vellego, and P. Metra, Appl. Phys. Lett. **67**, 3189 (1995).
[13] J. R. Clem, M. Benkraouda, T. Pe, and J. McDonald, Chin. J. Phys. **34**, 284 (1996).
[14] W. T. Norris, J. Phys. D **3**, 489 (1970).
[15] E. H. Brandt and M. Indenbom, Phys. Rev. B **48**, 12 893 (1993).
[16] E. Zeldov, J. R. Clem, M. McElfresh, and M. Darwin, Phys. Rev. B **49**, 9802 (1994).
[17] D. E. Oates, A. C. Anderson, and P. M. Mankiewich, J. Supercond. **3**, 251 (1990).
[18] C. C. Chin, D. E. Oates, G. Dresselhaus, and M. S. Dresselhaus, Phys. Rev. B **45**, 4788 (1992).
[19] A. T. Findikoglu, D. W. Reagor, P. N. Arendt, S. R. Foltyn, J. R. Groves, Q. X. Jia, E. J. Peterson, L. Boulaevskii, and M. P. Maley, (unpublished).